THE AUTHORS

C. G. Moyers, Jr. has worked in the Engineering Department of Union Carbide since 1956 with time off to obtain a Ph.D. at Delaware in 1971. He has been chasing solid particles through Union Carbide's crystallizers, centrifuges, and dryers for about 10 years. (When not tracking crystals, he can be found in pursuit of tennis balls.)

Alan Randolph received his Bachelor of Science in Chemical Engineering from the University of Colorado in 1956 and the Masters and Ph.D. from Iowa State in 1959 and 1962. He has since spent five years in industry and eight years in academia where he is currently Professor of Chemical Engineering at the University of Arizona, Tucson. Alan first got hooked on the unit operation of crystallization some fifteen years ago and has been an addict ever since. He is coauthor of a recent book on crystallization *Theory of Particulate Processes* with M. A. Larson.

Alan spends his winters in the Arizona sunshine and his summers in the cool pines at Los Alamos, New Mexico, where he has served as Visiting Staff Member at the Los Alamos Scientific Laboratory for the past seven summers.

Bubble-Free Expansion of Gas-Fluidized Beds of Fine Particles

G. DONSÌ and L. MASSIMILLA

Istituto di Chimica Industriale e Impianti Chimici, Università
Laboratorio di Ricerche sulla Combustione, CNR
Naples, Italy

Five different fine powders with average particle size of about 100 microns or smaller were fluidized with air over their respective bubble-free ranges of fluidization. Photographs taken through the front transparent wall of the column showed that the beds contained cavities and microchannels whose sizes were of the same order of magnitude as the particle size. It is shown that interparticle van der Waals and capillary forces play an important role in the bubble-free expansion of small particles. Measurements of bed expansion and average particle drag coefficients are consistent with the proposed role of interparticle forces.

SCOPE

Fine catalytic powders, less than 100μm in size, are widely used in industry for fluid bed operations because of their high contact areas and favorable heat transfer rates. Contrary to beds of coarser materials, beds of fine particles can be bubble-free fluidized over a considerable range of superficial velocity and expanded to voidages as high as 0.60 to 0.65 before bubbles appear. This expansion of the dense phase may affect solids mobility in the bed, gas exchange processes, and particle renewal at heat transfer surfaces.

The problem of whether a bed of particles fluidizes in a particulate or aggregative manner has long been of concern to chemical engineers (Wilhelm and Kwauk, 1948; Trawinski, 1953). It has been suggested (Anderson and Jackson, 1964) that aggregative fluidization results from the instability of the state of uniform fluidization to small perturbations. However, Molerus (1967) has shown that not all gas fluidized beds are unstable, especially for low voidages, fine particles and low particle to fluid density ratios. The range of bubble-free fluidization found for particles smaller than about 100μm (Davies and Richardson, 1966; Rietema, 1967; Geldart, 1967; Rowe, 1969) is in general agreement with this conclusion. Very fine particles do not show particulate behavior, however (Baerns, 1966). Instead, heavy channeling prevails, probably because of pronounced interparticle forces.

The work described in this paper is an extension of earlier work (Massimilla et al., 1972) aimed at elucidating the structure and mechanisms of bubble-free gas fluidized beds.

CONCLUSIONS AND SIGNIFICANCE

Previous conclusions (Massimilla et al., 1972) regarding bubble-free fluidization of cracking catalysts have been shown to be valid for a number of different powders. In particular, it has been shown that bubble-free fluidized beds contain cavities and microchannels. Particles show little mobility, and average drag coefficients were higher and permeabilities lower than for comparable liquid fluidized beds. Expansion of beds of fine particles occurs primarily by the nucleation and growth of cavities or particle defects.

The above mode of bed expansion has been explained by considering the role of interparticle forces, in particular, van der Waals and capillary forces. These forces act to stabilize cavities and microchannels. The cavity growth mechanism of bed expansion probably occurs because of a broad distribution of interparticle forces due

to widely differing surface asperities. Calculations indicate that interparticle forces are at least of the same order of magnitude as particle weights so that interparticle forces, together with gravity and drag forces, play an important role in determining the fluidization behavior of fine powders.

EXPERIMENTAL APPARATUS AND PROCEDURE

The experiments were carried out in a 150-mm diam. semicircular column as described previously (Massimilla et al., 1972). This shape was chosen so that the bed would have one flat wall suitable for observation while the number of sharp corners, potential promoters of bubbles, would be minimized. The column could be inclined up to 2° to the vertical. Plane parallel optical glass was used in order to obtain accurate measurements.

The relevant physical properties of the solids used are presented in Table 1. The tabulated mean particle diameter $\overline{D_p}$ is the mean aperture diameter for the sieves between which the particles were collected or the surface mean diameter depending on the breadth of particle size in the powder. Particle sphericities were evaluated from samples of about 100 particles. Particle surfaces, viewed through an electron scanning microscope at a magnification of 20,000 generally appeared to be corrugated. For the Ludox catalyst material, only spheroidal protuberances could be observed and the size distribution of these protuberances is given in Table 2.

The fluidizing fluid for the experiments was air fed from a pressurized cylinder. Since solids mobility is very limited in bubble-free fluidization, electrostatic charges are not expected to develop during the experimental runs. However, the bed was bubbled before each run, and consequently the incoming air was humidified (except for the experiments with sodium bicarbonate) to dissipate electrostatic charges. The surface water, although sufficient to promote surface electrical conductivity, is not expected to cause substantial interparticle forces because of the thinness of the sorbed layer (Rumpf, 1958).

Unexpanded bed heights were between 20 and 25 cm. The bed was first bubbled, after which the air flow rate was reduced well below the point of incipient fluidization and then increased to the desired value. The minimum fluidization velocity U_{mf} was defined as the superficial air velocity at which the pressure drop across the bed equalled the weight of bed material per unit area. The minimum bubbling velocity U_{mb} defined as the point at which the first bubble appeared, was much less reproducible than U_{mf}, probably due to the influence of column geometry and the unevenness of gas distribution on the behavior of the bed as U approaches the minimum bubbling condition. Pressures measured at different levels showed that the pressure varied linearily with height. This suggests that the average bed voidage is independent of height and that particle segregation can be neglected (at least over the time required for a run). In any case, micrographs were always taken at two or more levels.

Still and motion pictures of cavities and microchannels were obtained as in the previous study (Massimilla et al, 1972). Again, only cavities with areas greater than D_p^2 were considered where $D_p = \overline{D_p}$ for the narrow cut materials and D_p was taken as the smaller limit of particle size for the broader size materials. Blurring of cavity boundaries due to remarkable transparency of particle aggregates made quantitative measurements difficult for the Ludox catalyst and impossible for sodium bicarbonate. Particle velocities were obtained by measuring with a stopwatch the time required for particles (observed through a magnification device) to traverse a known distance.

EXPERIMENTAL RESULTS

Results are presented here not only for the materials listed in Table 1 but also, for purposes of comparison, for the Ketjen catalyst studied previously. Except where otherwise specified, data from the previous study are indicated with open circles.

Bed Structure

Fractional cavity surface areas a_{ca} and average cavity sizes $\overline{A}_{ca}/D_p^2$ determined at the wall are shown in Figures 1 and 2 as functions of U/U_{mf}. The values for the Ludox catalyst are lower than expected even though ϵ_{mf} and ϵ_{mb} (see Table 1) are the same as for Ketjen catalyst of the same size. This probably arises from the difficulties in reading cavity areas for this material as mentioned above. The results for all materials can be correlated by the equations

$$a_{ca} = 0.105\, U/U_{mf} - 0.034 \qquad (U/U_{mf} > 1) \quad (1)$$

$$\overline{A}_{ca}/D_p^2 = 0.92\, U/U_{mf} + 0.63 \qquad (U/U_{mf} > 1) \quad (2)$$

with mean deviations of 0.042 and 0.36, respectively.

TABLE 1. CHARACTERISTICS OF SOLIDS USED IN THE EXPERIMENTS

Batch		Sieve size, μm	Particle sphericity	Particle specific gravity	ϵ_{mf}	U_{mf} m s^{-1}	ϵ_{mb}	U_{mb} m s^{-1}	Particle surface characteristics
Alumina catalyst	△	176-76 $\overline{D_p} = 90$	0.88	1.55	0.58	0.0076	0.61	0.0141	Slightly corrugated with a dense coverage of irregular excrescences
PVC	▽	176-76 $\overline{D_p} = 105$	0.98	0.98	0.50	0.0066	0.55	0.0125	Strongly corrugated
Ludox Silica catalyst	◇	104-76 $\overline{D_p} = 90$	0.99	1.51	0.55	0.0029	0.63	0.0069	Smooth, with a light coverage of spheroidal protuberances
Ammonoxidation catalyst	□	104-76 $\overline{D_p} = 90$	0.99	1.49	0.46	0.0044	0.50	0.0072	Corrugated with a coverage of excrescences
Sodium bicarbonate	+	76-61 $\overline{D_p} = 68$	0.92	2.20	0.48	0.0033	0.52	0.0054	—

The cavity number density $N_{ca}\frac{(1-\epsilon_{mf})}{(1-\epsilon)}$ appears to go through a step change at about $U/U_{mf}=1$ and then remains nearly constant thereafter as shown in Figure 3. The average number density is then given by

$$N_{ca}D_p^2\frac{1-\epsilon_{mf}}{1-\epsilon}=7.1\times10^{-2} \qquad (3)$$

Cavity size distributions were found to be of logarithmic normal type as shown in Figure 4. Logarithmic standard deviations and means of these distributions are in agreement with the correlations presented by Massimilla et al. (1972) for Ketjen catalyst. Cavities were again elongated in shape with the ratio of major to minor axes (L_{ca}/l_{ca}) log-normally distributed (see Figure 5). The standard deviation and mean were also in good agreement with earlier results for the Ketjen catalyst. For the Ludox catalyst, log ($A_{ca}/\overline{A_{ca}}$) and log (L_{ca}/l_{ca}) were strongly correlated (correlation coefficient of 0.8), whereas correlation for the other materials was negligible. As in the previous study, only about 20% of cavities had their major axes orientated vertically.

Microchannels were observable in the upper half of the particulate fluidization range, that is, for $(U_{mf}+U_{mb})/2<U<U_{mb}$. These microchannels act as spouts raising particles within the bed but not breaking the bed surface. The size, density, and life time of these microchannels were similar to those observed for the Ketjen catalyst at U approaching U_{mb}. In particular, the gas flow through these microchannels constitutes only a small fraction of the total gas flow rate. With alumina catalyst microchannels often ended with a chain of small bubbles.

TABLE 2. SURFACE PROTUBERANCES OBSERVED FOR LUDOX CATALYST

Protuberance diam., micron	0.05	0.10	0.15	0.20	0.25	0.30	>0.30
Relative frequency	0.16	0.20	0.22	0.21	0.12	0.05	0.04

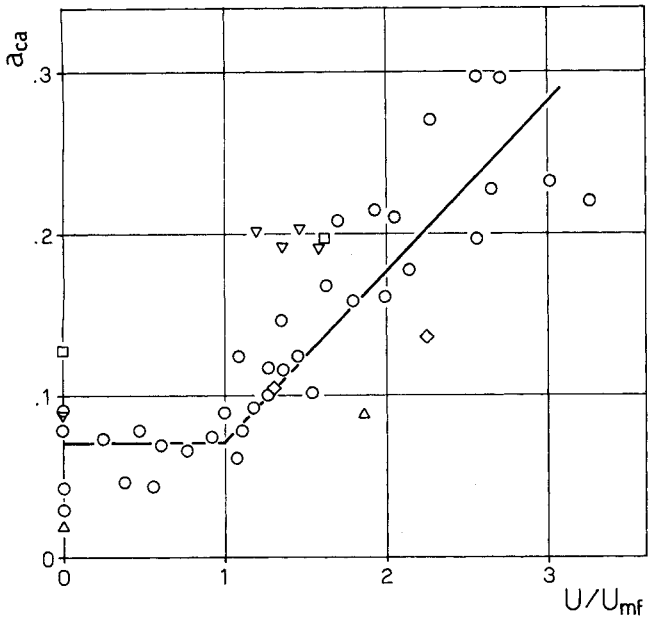

Fig. 1. Surface void fraction vs. U/U_{mf}. In this and following figures ○ = Ketjen catalyst. Other symbols as in Table 1.

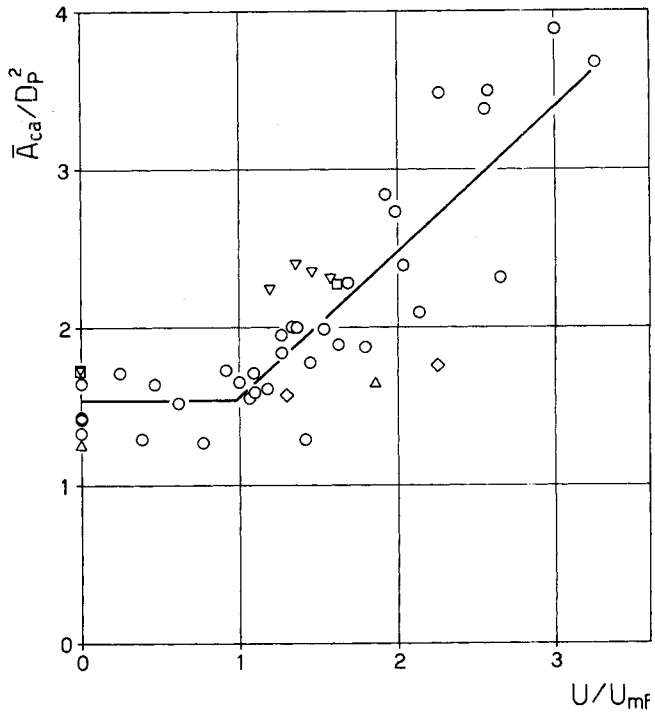

Fig. 2. Average cavity size vs. U/U_{mf}.

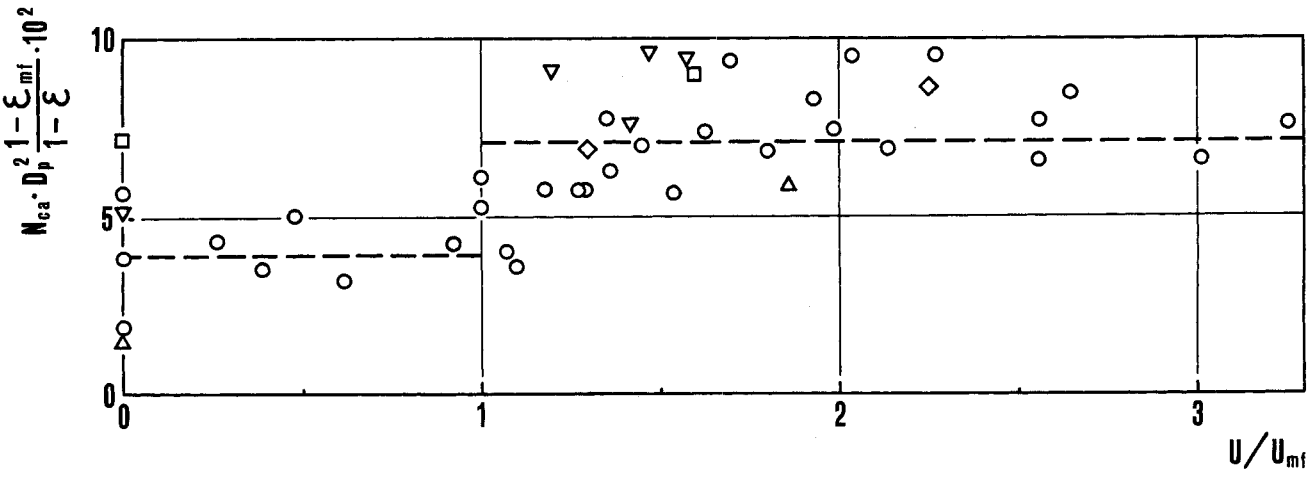

Fig 3. Cavity density vs. U/U_{mf}.

Solids Mobility

In the previous study with Ketjen catalyst, particle motion at the wall was found to be very limited and directed only downwards. Particle velocities are plotted in Figure 6 as a function of U/U_{mf}. For PVC particles and ammonoxidation catalyst, particles were found to be stationary throughout the bubble-free range of fluidization. In other cases, particle motion occurred only for $U > (U_{mf} + U_{mb})/2$. Even at $U \approx U_{mb}$, however, downwards velocities never exceeded $0.06U$. By comparison, particle velocities of 0.3 to $0.5U$ have been measured for liquid-fluidized beds at similar values of bed expansion and of U/U_{mf} (Carlos and Richardson, 1968; Volpicelli et al., 1966). Downwards solids motion appeared to be closely related to changes in cavity size, shape, and orientation. There is a similarity between the displacement of horizontally elongated cavities in this study and the travel of voidage waves through liquid fluidized beds (Slis et al., 1959).

It may be noted that solids mobility occurs mainly for the channeling range of U/U_{mf} and that both particle velocity and microchannels have a pulsatory character. This suggests that downwards solid motion may balance transport of solids in microchannels near the wall.

Bed Expansion and Drag

The pressure drop versus superficial gas velocity data for this study fitted closely the classical intersecting Δp vs. U straight lines for smooth fluidization. Similar patterns were obtained by Davies and Richardson (1966) and by Massimilla et al. (1972) for other powders. Each material tested had its own range of bubble-free fluidization. The Richardson and Zaki (1954) correlation for solid-liquid systems

$$U = U_0 \epsilon^n \qquad (4)$$

also describes the expansion of bubble-free gas fluidized beds. Expansion indices n are plotted in Figure 7 as a function of the Galileo number. For comparison, values

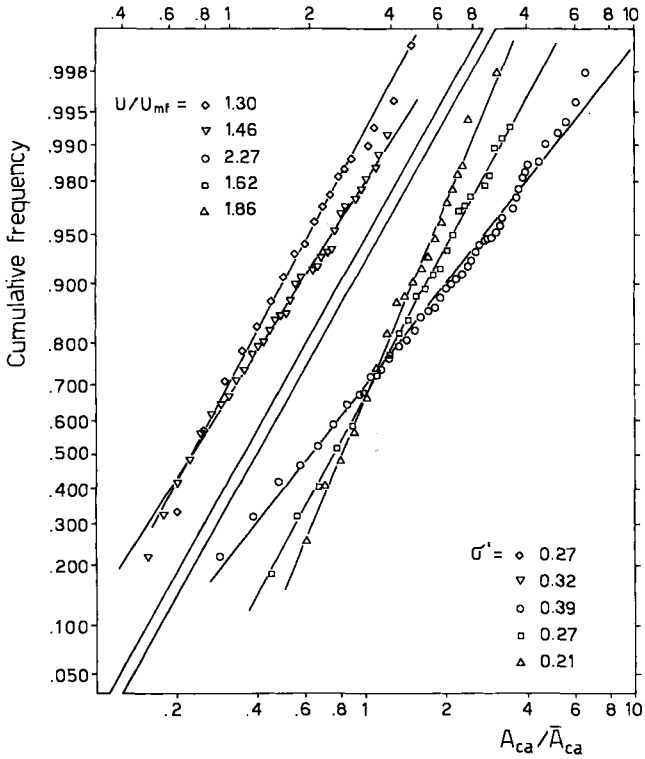

Fig. 4. Typical logarithmic normal distributions of cavity sizes. σ' = standard deviation.

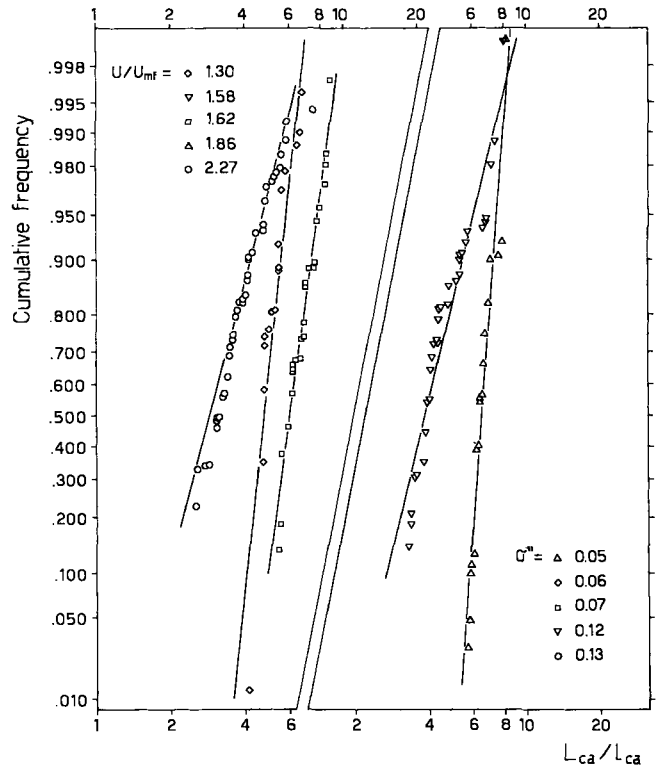

Fig. 5. Typical logarithmic normal distributions of ratios of cavity major to minor axis. σ'' = standard deviation.

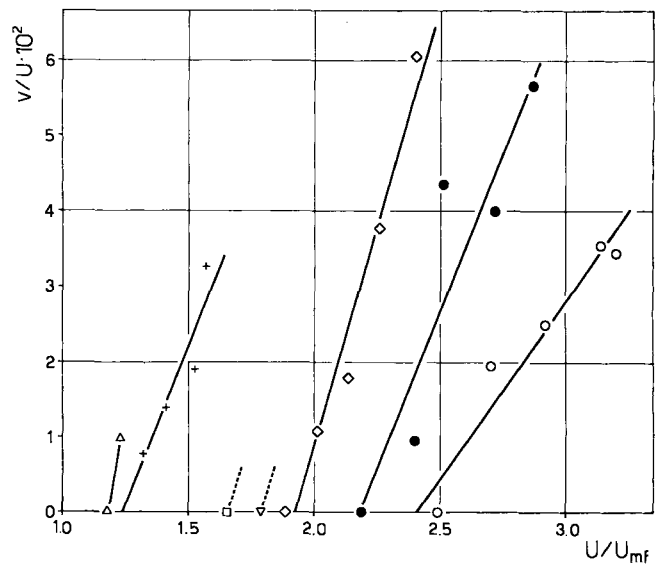

Fig. 6. Downward particle velocity at the wall as a function of U/U_{mf}: ○ = 40-45 μmKetjen catalyst; ● = 40-176 μmKetjen catalyst. Other symbols as in Table 1.

of n found for liquid-fluidized beds (Richardson and Zaki, 1954) or for particulate gas fluidized systems of relatively coarse spheres (Ergun and Orning, 1949; Richardson, 1971) are also presented in Figure 7.

Overall drag coefficients C_D are shown in Figure 8 together with C_D versus Re correlations for liquid fluidized beds (Richardson and Zaki, 1954) and for fixed arrays of spheres (Gunn and Malik, 1966, 1967) having cubic, orthorhombic, and rhombohedral configurations. For the arrays of spheres, voidage was varied by increasing the distance between planes or by expanding the sphere spacing in planes normal to the direction of flow.

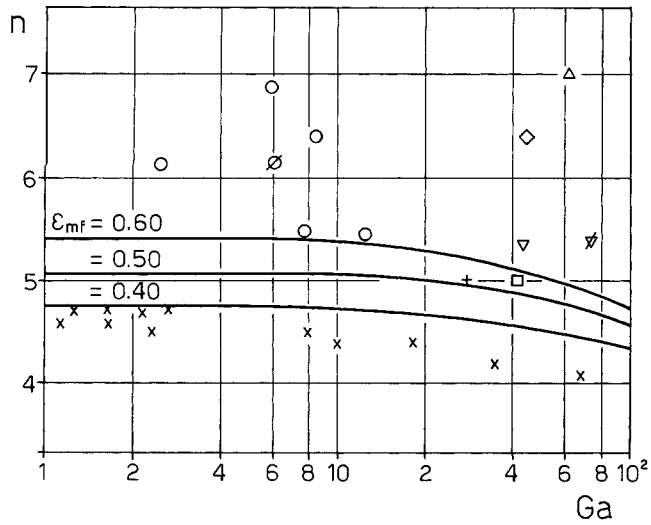

Fig. 7. Expansion index n, Equation (4). vs. Galileo number: ⌀—cracking catalyst; ⌀—PVC; ×—liquid-fluidized beds (Ergun and Orning, 1949; Richardson and Zaki, 1954; Richardson, 1971). Lines from Ergun equation and Equation (4).

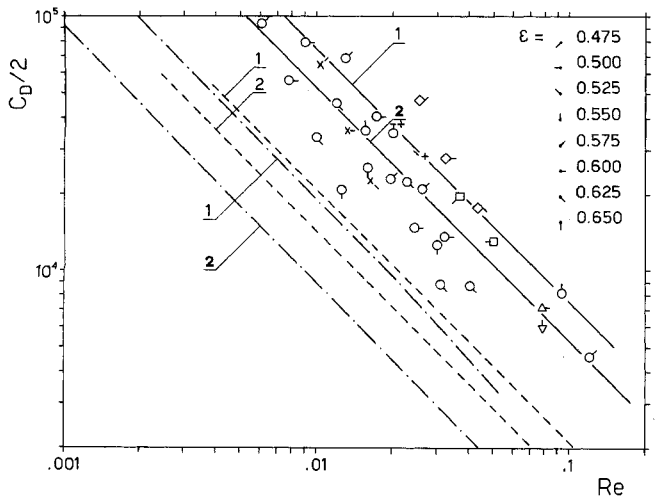

Fig. 8. Drag coefficient vs. *Re* at different voidages: ×—cracking catalyst; – – – – – Richardson-Zaki correlation line (1) $\epsilon = 0.55$; (2) $\epsilon = 0.65$; ——— Experimental data (Gunn and Malik, 1966); – – – – – – – interpolated from Gunn and Malik data

Line	Assembly	Interplanar spacing	Intersphere spacing	Void fraction range
——1	body centered	1.0	1.0	0.476
——2	cubic	1.0-2.0	1.0	0.476-0.738
– – –1	cubic	1.0	1.15	0.60
– – –2	cubic	1.0	1.23	0.65

DISCUSSION

Experimental results for the materials listed in Table 1 are essentially in agreement with those obtained earlier for Ketjen catalyst. It appears likely that the phenomena of cavity nucleation and growth observed at the wall should extend into the interior of the bed, at least in a qualitative sense.

Figure 9 shows some possible packing configurations at the wall and inside an unfluidized bed of spherical particles. Dotted lines mark elementary cells. Because of the tendency of the wall to prevent ordinate packing, cells like c are expected to predominate at the wall, and this type of cell has been considered in relation to studies of wall effects for packed beds (Sonntag, 1960). For viscous flow the relative permeability for packing *a* to that of cells of type c is 1.0 to 1.2 (Reboux, 1954) so that drag at the wall is not expected to differ greatly from that experienced by interior particles. One particle wall defects *d'* and *d''* are also shown in Figure 9. The existence of such defects for $U/U_{mf} < 1$ is dependent on the ability of the wall to support the structure. Such wall defects are probably the major cause of discrepancy between behavior at the wall and in the bed interior.

Certainly, wall observations indicate that a fluidized bed reacts to increases in gas velocity by developing void spaces rather than by uniform bed expansion. The increase in cavity area at the wall (see Figure 1) results from the nucleation of new cavities at $U \approx U_{mf}$ and to the enlargement of existing cavities for $U > U_{mf}$ (see Figures 2 and 3). The skewness of the cavity size and major to minor axis ratio distributions (Figures 4 and 5) shows further the nonuniformity of bed expansion. The logarithmic-normal distribution of $A_{ca}/\overline{A}_{ca}$ suggests that large cavities tend to grow most with increasing gas flow rate (Hald, 1967; Massimilla et al., 1972). It is possible then that microchannels result from the growth of larger cavities which have their major axes orientated vertically.

The relatively high values of n and C_D shown in Figures 7 and 8 indicate that bubble-free gas fluidized beds have lower permeabilities than liquid-fluidized beds or gas-fluidized beds of coarser materials. This is consistent with the appearance of unconnected cavities which tend to cause average drag coefficients to be greater than for particles in uniformly spaced assemblies (Rowe and Henwood, 1961). The small degree of solids mobility (see Figure 6) is consistent with the appearance of cavities

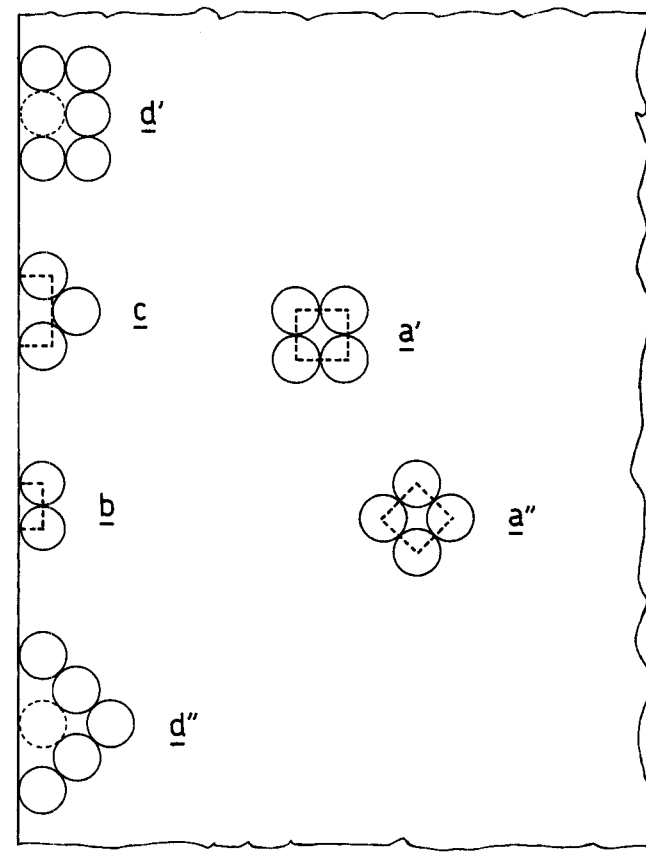

Fig. 9. Wall and midbed packings of spheres.

and the low bed permeabilities.

Taken altogether, these observations lead us to postulate that interparticle forces are playing a major role in stabilizing the bed structure for bubble-free gas fluidized beds. The origin of such forces may be due to: (1) van der Waals forces, (2) forces due to surface tension of sorbed moisture, and (3) electrostatic forces. Electrostatic forces are disregarded here because of the experimental precautions described earlier.

The van der Waals force of attraction between a particle and a semi-infinite slab is (Hamaker, 1937; Krupp, 1967)

$$F_w = \frac{h\omega}{8\pi z_0^2} R\left[1 + \frac{h\omega}{8\pi^2 z_0^3 H}\right] \tag{5}$$

Here we arbitrarily assume that the minimum separation distance between the surfaces is given by $z_0 = 4$Å, a value slightly in excess of the lattice constant of weakly van der Waals bonded molecular crystals. The term in the bracket accounts for deformation of the interface between adherents. Equation (5) also gives the cohesion force between two perfectly spherical particles of radii R_1 and R_2 if we substitute

$$R = \frac{R_1 R_2}{R_1 + R_2} \tag{6}$$

Sorption of water at the interface between interacting particles gives rise to a force of attraction which can be written (Rumpf, 1958; Schubert, 1972):

$$F_c = 4 C \sigma R \tag{7}$$

where σ is the surface tension (assumed as a first approximation to be equal to that between pure water and air) and C is a dimensionless factor which depends on the amount of sorbed water, the geometry of the water bridges, and the distance between adherents. For particles in contact, that is, when the interparticle separation is about z_0, C is about 2.5. C decreases rapidly with increasing z/R until $C = 0$ as bridge breakup occurs for $z/R \approx 0.05$ (Schubert, 1972).

The sharp drop in interparticle attraction as interparticle separation increases suggests that the work required to uniformly expand a bed would be considerably larger than that required for growth of concentrated voids. The appearance of cavities and microchannels can be explained on this basis. Detailed calculations for van der Waals forces are presented in the Appendix.

Equations (5) to (7) also show that both van der Waals and capillary forces between two spheres differ at most by a factor of 2 from the corresponding forces between a sphere and a semi-infinite slab. In view of the large spread of forces between individual particles, the assumption that the glass wall should not greatly affect the observations would appear to be reasonable.

To estimate the order of magnitude of F_w, we must first estimate the different terms in Equation (5). Based on assumptions in previous work (Krupp, 1967), we estimate the van der Waals-Lifshitz constant to be about 2eV, intermediate between values for polymers and metals. Values of H of 10^8 to 10^9 N/m^2 are estimated for catalysts, whereas the value for PVC should be in the range 10^5 to 10^6 N/m^2. Thus the second term in the bracket of Equation (5) is negligible compared with unity and interparticle forces are of order 10^{-6} N for particles of 40 to 100μm in size. This value may be compared with particle weights which range between 10^{-9} and 10^{-8} N. The difference between the van der Waals force and weight is even more marked for PVC. At the same time, Equation (7) predicts capillary forces of about 10^{-5} N for particles of the given size range.

The above discrepancies between these interparticle forces and particle forces appear to be unlikely in view of the relatively smooth fluidization achieved for each of the powders studied. The above estimates of van der Waals and capillary forces are based on sphere radii. In reality, electron microscope observations have shown that protuberance radii R' are much smaller than the particle radii. Quantitative measurements of the R' distribution were only possible for the Ludox catalyst as noted earlier, and these measurements can be used to account for the influence of protuberances (Krupp and Sperling, 1965). Replacing R by $R' = 10^{-7}$ m (see Table 2), setting $H = 10^8$ to 10^9 N/m^2 and assuming a few layers of sorbed water, we estimate interparticle forces to be of the same order of magnitude as particle weight.

We note that the magnitude of interparticle attraction forces may change by two or three orders of magnitude depending on the values of R'. Since R' covers a broad range, particles are expected to differ widely in how they respond to an increase in gas velocity tending to separate them. Particles subject to weak attractive forces will tend to separate (causing cavity nucleation or enlargements). This will continue in the direction of least resistance. Cavity growth may stop if the surrounding solids aggregate is brought to a state of higher stability. Since the number of contact points with sufficiently small R' is relatively small, it is expected that cavities should grow at a relatively small number of positions in the bed. This is in accord with the observations of this paper (for example, see Figure 3). The above considerations are also consistent with the energy calculations given in the Appendix and with the constancy of cavity density for $U/U_{mf} > 1$.

This discussion concerns the role of particle weight, drag and interparticle (van der Waals and capillary) forces on the behavior of fine powders in the bubble-free range of fluidization. No attempt has been made to distinguish between different materials. Under the controlled experimental conditions studied in this work, differences between powders were minor, more or less within the range of the scatter of the data. It must be noted, however, that in practice changes of such factors as R' and H due to variations in temperature, relative humidity, concentration of reacting species, particle attrition, coating or fouling may cause F_c and F_w to change by orders of magnitude. It is significant, however, that changes in the drag/voidage relations, solids mobility, and bed structure observed between bubble-free gas fluidization and liquid fluidization are consistent with the appearance of capillary forces and expected magnification of van der Waals forces for the gas-fluidized case.

ACKNOWLEDGMENT

The assistance of Miss C. Zucchini in carrying out experimental work is gratefully acknowledged. The authors are also indebted to Professor H. Krupp for discussion and to Dr. I. R. Grace for discussion and for rewriting the paper in the *AIChE Journal* format.

NOTATION

a_{ca} = void fraction at the wall
A_{ca} = cavity area, m^2
$\overline{A}_{ca}$ = average cavity area, m^2
C = dimensionless factor in Equation (7)

C_D = average drag coefficient for particle assembly
D_p, $\overline{D_p}$ = particle diameter, m
F_c = capillary force, N
F_w = van der Waals force, N
Ga = Galileo number, $\rho_f(\rho_p - \rho_f)g\overline{D_p}^3/\mu^2$
H = hardness, N m^{-2}
$h\omega$ = Lifshitz-van der Waals constant, J
l_{ca} = minor axis of cavity, m
L_{ca} = major axis of cavity, m
n = expansion index, Equation (4)
N_{ca} = number of cavities per unit area at the wall, m^{-2}
R = radius of curvature at point of contact, m
R_1, R_2 = sphere radii, m
R' = radius of curvature of an asperity, m
Re = particle Reynolds number, $\overline{D_p}U\rho_f/\mu$
U = superficial fluid velocity, m s^{-1}
U_0 = terminal velocity, m s^{-1}
v = particle downwards velocity at the wall, m s^{-1}
W_{ca} = work required to expand an array of particles by nucleation of one particle cavities, J kg^{-1}
W_{us} = work required to expand an array of particles uniformly, J kg^{-1}
z = distance between adherents, m
z_0 = minimum distance between adherents, m

Greek Letters

ϵ = voidage
ϵ_0 = voidage of an array of spheres for a mean particle separation of z_0
μ = fluid viscosity, kg m^{-1}s^{-1}
ρ_f = fluid density, kg m^{-3}
ρ_p = particle density, kg m^{-3}
σ = surface tension, N m^{-1}

Subscripts

mb = minimum bubbling
mf = minimum fluidization

LITERATURE CITED

Anderson, T. B., and R. Jackson, "The nature of aggregative and particulate fluidization," *Chem. Eng. Sci.*, **19**, 509 (1964).

Baerns, M., "Effect of interparticle adhesive forces on fluidization of fine particles," *Ind. Eng. Chem. Fundamentals*, **5**, 508, (1966).

Carlos, C. R., and J. F. Richardson, "Solids movement in liquid fluidized beds," *Chem. Eng. Sci.*, **23**, 813 (1968).

Davies, L., and J. R. Richardson, "Gas interchange between bubbles and the continuous phase in a fluidized bed," *Trans. Instn. Chem. Engrs.*, **44**, 293 (1966).

Ergun, S., and A. A. Orning, "Fluid flow through randomly packed columns and fluidized beds," *Ind. Eng. Chem.*, **41**, 1179 (1949).

Geldart, D., Discussion on paper by Rietema, *Proc. Intern. Symp. Fluidization*, p. 170, Eindhoven (1967).

Gunn, D. J., and A. A. Malik, "Flow through expanded beds of solids," *Trans. Instn. Chem. Engrs.*, **44**, 371 (1966).

Gunn, D. J., and A. A. Malik, "The structure of fluidized beds in particulate fluidization," *Proc. Intern. Symp. on Fluidization*, p. 52, Eindhoven (1967).

Hald, A., *Statistical Theory with Engineering Applications*, Wiley, New York (1967).

Hamaker, H. C., "The London van der Waals attraction between spherical particles," *Physica IV*, No. 10, 1058 (1937).

Krupp, H., "Particle adhesion," *Advan. Colloid Interface Sci.*, **1**, 111 (1967).

———., and G. Sperling, "Haftung kleiner Teilchen von Feststoffen," *Z. für ang. Physik*, **19**, 259 (1965).

Massimilla, L., G. Donsi, and C. Zucchini, "The structure of bubble-free gas fluidized beds of fine fluid cracking catalyst particles," *Chem. Eng. Sci.*, **27**, 2005 (1972).

Molerus, O., "The hydrodynamic stability of the fluidized bed," *Proc. Intern. Symp. on Fluidization*, p. 134. Eindhoven (1967).

Reboux, P., *Phénomènes de fluidisation*, Assoc. Francaise de Fluidisation, Paris (1954).

Richardson, J. F., "Incipient fluidization and particulate systems," in *Fluidization*, J. F. Davidson and H. Harrison (eds.), Academic Press, London (1971).

———., and W. N. Zaki, "Sedimentation and fluidization," *Trans. Instn. Chem. Engrs.*, **32**, 35 (1954).

Rietema, K., "Application of mechanical stress theory to fluidization," *Proc. Intern. Symp. on Fluidization*, p. 154, Eindhoven (1967).

Rowe, P. N., "The delayed bubbling of fluidized beds of fine particles," *Chem. Eng. Sci.*, **24**, 415 (1969).

———., and G. A. Henwood, "Drag forces in a hydraulic model of a fluidized bed," *Trans. Instn. Chem. Engrs.*, **39**, 43 (1961).

Rumpf, H., "Grundlagen und Methoden des Granulierens," *Chem. Ing. Tech.*, **30**, 144 (1958).

Schubert, H., "Untersuchungen zur Ermittlung von Kapillardruck und Zugfestigkeit von feuchten Haufwerken aus körnigen Stoffen," Ph.D. dissertation, Univ. Karlsruhe (1972).

Slis, P. L., T. W. Willems, and H. Kramers, "The response of the level of a liquid fluidized bed to a sudden change in the fluidizing velocity," *Appl. Sci. Res.* **8A**, 209 (1958).

Sonntag, G., "Einfluss des Luckenvolumens auf den Druckverlust in gasdurchströmten Fullkorpersäulen," *Chem. Ing. Tech.*, **32**, 317 (1960).

Trawinski, H., "Effektive Zahigkeit und Inhomogenität von Wirbelschichten," *ibid.*, **25**, 229 (1953).

Volpicelli, G., L. Massimilla, and F. A. Zenz, "Nonhomogeneities in solid-liquid fluidization," *Chem. Eng. Progr., Symp. Ser., No. 67*, **62**, 42 (1966).

Wilhelm, R. H., and M. Kwauk, "Fluidization of solid particles," *Chem. Eng. Progr.*, **44**, 201 (1948).

APPENDIX

If the effect of deformations is neglected and a cubic arrangement of spheres is assumed, the separation work per unit mass of solids for uniform bed expansion can be derived by using Equation (5), that is,

$$W_{us} = \int_{z_0}^{z} F_w dz = \frac{9}{64}\,\frac{h\omega}{\pi^2\rho_p}\,\frac{1}{R^2}\left[\frac{1}{z_0} - \frac{1}{z}\right] \tag{8}$$

where

$$z \approx \frac{2R}{3}\,\frac{\epsilon - \epsilon_0}{1 - \epsilon} \tag{9}$$

Here ϵ_0 is the voidage for particles at the adhesional separation z_0, so that ϵ_0 can be taken as 0.476, the voidage for packed beds having a cubic arrangement.

The separation work for bed expansion from ϵ_0 to ϵ with the formation of unconnected one-particle cavities is

$$W_{ca} = \frac{9}{64}\,\frac{h\omega}{\pi^2\rho_p}\,\frac{1}{R^2 z_0}\,\frac{\epsilon - \epsilon_0}{1 - \epsilon} \tag{10}$$

From Equations (8), (9), and (10),

$$\frac{W_{us}}{W_{ca}} = \frac{1 - \epsilon}{\epsilon - \epsilon_0}\left\{1 - \frac{z_0}{\frac{2R}{3}\,\frac{(\epsilon - \epsilon_0)}{(1 - \epsilon)}}\right\} \tag{11}$$

so that

$$\frac{W_{us}}{W_{ca}} \approx \frac{1 - \epsilon}{\epsilon - \epsilon_0} \tag{12}$$

where ϵ is only slightly in excess of ϵ_0. Equation (12) indicates that the uniform expansion work is greater than that required to expand the bed nonuniformly, at least for the range of ϵ of interest. The above conclusion can be extended to cavities or defects of more than one particle.

Manuscript received January 9, 1973; revision received June 21 and accepted July 3, 1973.